Published in Sensors and Actuators A: Physical 142, issue 1, 284-291, 2008
which should be used for any reference to this work

Reliability improvement of suspended platinum-based micro-heating elements

J. Courbat *, D. Briand, N.F. de Rooij

Institute of Microtechnology, University of Neuchâtel, Rue Jaquet-Droz 1, P.O. Box 526, CH-2002 Neuchâtel, Switzerland

Abstract

Micro-hotplates consisting of a platinum-based heating element embedded in two low-stress silicon nitride layers were fabricated. In this communication, we report on the composition of the heater and its influence on both the micro-hotplate's life expectancy and the highest reachable operating power. These factors were characterized by measuring the deformation of the membrane, by ramping up the power until breakdown and by performing accelerated aging tests. Finally, the failure mechanisms were investigated using optical and SEM observations. The type of material used as adhesion layer has a strong influence on the heating element's performances. Addition of iridium significantly improved the lifetime of the device.

Keywords: Platinum; Iridium; Heater; Micro-hotplate; Material; Reliability; Aging

1. Introduction

Over the years, micro-hotplates have shown to be suitable for different type of microsystems such as actuators, flow sensors, gas sensors, infrared sources, and micro-thrusters [1–4]. Such devices combine low power consumption, fast thermal transient response and easy manufacturing process. Papers referring to micro-hotplates in the literature were mainly focused on the applications and on the optimization of their thermal behavior based on FEM simulations [2,5]. Since such components generally aim at functioning for several years before malfunction, for instance when used in gas sensors for the automotive industry, their reliability is one of the most relevant aspect to consider and optimize.

The work reported on the reliability of micro-hotplates was mainly concentrated on the thermal and mechanical behavior of the devices. Simulations models and accelerated aging test protocols were developed to investigate the failure mechanisms in order to optimize the reliability of the devices [6–10]. The investigations have shown that platinum-based micro-heaters are more robust than those made of polysilicon when devices have to operate at relatively high temperature. A major drawback of polysilicon-based heater is their long term drift of their electrical resistance occurring at high temperature [11,12]. In CMOS technology, it has been replaced by the use of MOSFET transistors as heating element [13]. The studies performed on the reliability of platinum-based heating elements are limited. Most of the studies dealing with the stability and reliability of the platinum-based metallizations referred to the Pt–Ti system, with only a few on the Pt–Ta system [14–19]. They report on the materials aspect of the platinum metallization for specific adhesion layers. The use of Ta as adhesion layer has the advantage over Ti to be compatible with the deposition of LPCVD Si_3N_4, providing hotplates with more robust membranes, and to diffuse less in platinum. The influence of the temperature during the processing or post-processing on the microstructural, electrical and mechanical properties of Pt–Ta-based metallizations has already been presented [15,17,18], as well as the degradation of Pt–Ta-based micro-heater operating at high temperatures [7,8,10,18].

In this work, the optimization of the material composition of platinum–tantalum-based heaters was investigated in order to increase the life expectancy and the maximum reachable operating temperature of micro-hotplate devices. The thickness as well as the composition of the tantalum-based adhesion layer has shown a significant influence on the platinum heaters' per-

* Corresponding author.
E-mail address: jerome.courbat@unine.ch (J. Courbat).

formances. Addition of iridium to the platinum has led to an improvement of the reliability of the micro-hotplates owing to the higher resistivity value of the heater metallization and, hence, to the lower current density required to reach a given temperature.

2. Design and fabrication

The micro-hotplate consists of a platinum double meander heater, which is embedded in two low-stress LPCVD silicon rich nitride (Si_xN_y) films that form the thermally insulated membrane. The membrane and the heater areas are $1 \times 1\,mm^2$ and $450 \times 450\,\mu m^2$, respectively (Fig. 1). An example of heating element is presented in Fig. 2. The width of the platinum line becomes wider in the center of the micro-hotplate to decrease the current density and thus the temperature. This aims at having a more uniform temperature over the whole heated area of the device, which is of important in the field of gas sensing for instance [10].

The fabrication began with the deposition by LPCVD of a 250-nm thick, low-stress silicon nitride layer on a 100-mm wide, 390-μm thick, (1 0 0) oriented silicon wafer. Then, the materials composing the heaters were deposited by e-beam evaporation which eased the patterning by using standard photolithography technique and lift-off process. As all the heating element materials can be deposited during the same fabrication step, a combination of several materials to be deposited can be investigated without extending the fabrication process. Four compositions were considered, referred to as PtTaThin, PtTaThick, PtTaSi and IrPtTa.

With the goal of investigating the influence of the adhesion layer thickness on the heater's performances, devices with two different adhesion film thicknesses were fabricated. PtTaThin consisted of an adhesion layer of 5 nm of Ta deposited onto the first layer of LPCVD Si_xN_y whereas PtTaThick was composed of a thicker adhesion film of 15 nm of the same material. These adhesion layers were covered with, respectively, 235 nm and 225 nm of platinum.

Some processing and especially post-processing steps can be performed at high temperature in air depending on the application targeted for the devices, among others we can mention the post-annealing of metal-oxide gas sensitive layers. These processes can lead to an oxidation of the tantalum layer which can cause the failure of the platinum film during the wire bonding of the device or its operation. With the aim of enhancing the reliability of the heater by delaying the oxidation of tantalum, we have investigated the possibility of incorporating tantalum silicide as adhesion layer instead of tantalum. Hence, oxidation of the tantalum will be lowered when exposed to high temperature and oxygen [20]. A layer of silicon was evaporated before the deposition of tantalum film and the formation of silicides occurred at 800 °C either during an annealing performed after the metal deposition or during the deposition of the second LPCVD of Si_xN_y. The silicon was deposited before the tantalum in order to avoid as much as possible the formation of platinum silicides, which can be unstable at temperatures higher than 700 °C [20]. In order to have all the tantalum reacting with the silicon during the silicide formation, an ideal ratio of Ta:Si of 1:2.21 is necessary [20]. Therefore, a 7-nm thick silicon film was deposited before the 3.5 nm of tantalum for the PtTaSi type of heating element. This adhesion layer was covered with 235 nm of Pt.

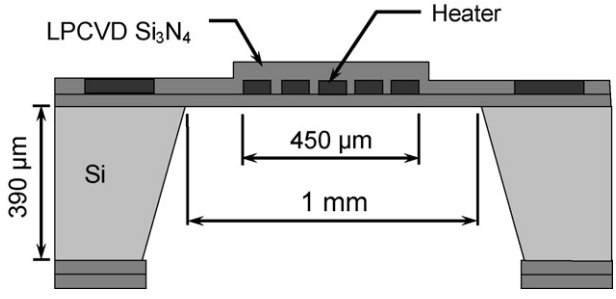

Fig. 1. Schematic cross-section view of the micro-hotplate chip. The heating element was embedded in two low-stress LPCVD Si_xN_y layers. The area of the heater and the membrane were $450 \times 450\,\mu m^2$ and $1 \times 1\,mm^2$, respectively.

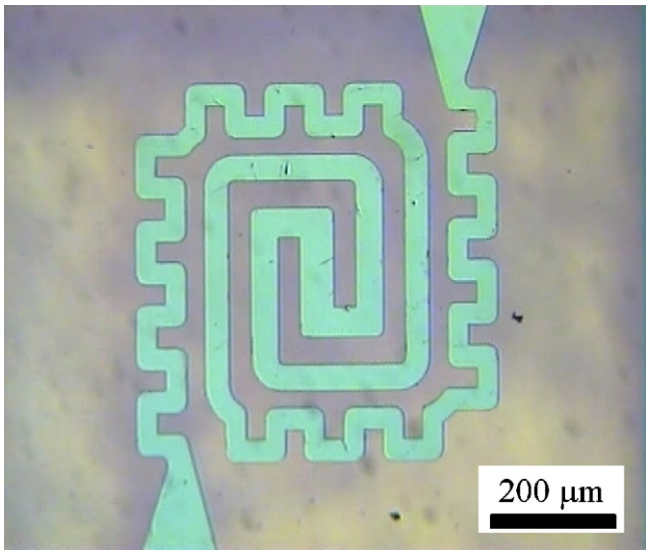

Fig. 2. Optical picture of the top view of a double meander Pt heater embedded in a low-stress LPCVD Si_xN_y membrane.

Electro-stress migration was the main failure mechanism of these micro-hotplates [8,10]. The last type of heater, IrPtTa, was designed to delay this effect by adding impurities at the platinum grain boundaries. According to the phase diagram of Pt–Ir [21], the maximum concentration for which iridium is soluble in platinum is slightly higher than 5%. Consequently, the 220-nm thick platinum film was covered with an 11-nm thick layer of iridium. It is expected that iridium diffused into the platinum during the deposition of the second LPCVD of Si_xN_y. The adhesion layer of IrPtTa was made of a 15-nm thick layer of tantalum.

Once the heating element was patterned, a second layer of 500-nm thick low-stress LPCVD Si_xN_y was deposited and patterned to allow later on wire bonding of the heater pads to a standard TO socket for characterization. Since the deposition of the latter is performed at high temperature, rearrangement of the atoms composing the heater film can take place. Therefore, formation of silicide and diffusion of the iridium and tantalum in, respectively, PtTaSi and IrPtTa occurred during this step.

Backside bulk micromachining of the silicon wafer was used to release the membrane. More details about the fabrication process can be found in reference [22]. Moreover, the two successive depositions of low-stress LPCVD Si_xN_y forming the membrane of the four heating element compositions were performed on all substrates in the same time in order the have exactly the same thickness and to reach the same temperature at a same input power.

3. Experimental

3.1. Characterization during processing

The thickness of the four heaters was measured by stylus profilometry (*Tencor*). Stress measurements of the four different compositions of platinum films and their sheet resistance have been measured during the whole fabrication process on wafers entirely covered with the films, without patterning the heating elements. These films were evaporated at the same time on these wafers and have passed through the same fabrication steps than those with the micro-heating elements patterned, ensuring the films to have the same properties. At the end of the fabrication process, the resistance values of the heating resistors were measured. Both optical and SEM observations, performed on the bonding pads of the heater, allowed us to investigate the influence of the material composition on the microstructure of the platinum-based heater.

3.2. Characterization of the devices in operation

3.2.1. Mechanical deformation

Optical profilometry (*UBM GmbH*) was used to monitor the membrane deformation as a function of both the input power and the type of heater.

3.2.2. Thermal measurements

To measure the temperature of the micro-hotplate as a function of the input power, a micro-thermocouple placed into contact with the heated surface was used. The micro-thermocouple was S type, made of Pt–PtRh wires with a diameter of 1.3 μm [23]. As already observed in previous calibration experiments on such devices, the heater resistance exhibited a linear behavior with temperature [22]. Therefore, the variation of the heater resistance was deduced by measuring its value at 0 and 120 mW, which corresponded to a variation of temperature of about 665 °C. This approximately was the highest power the device could withstand before non-linear behavior of the platinum-based heater leading to failure of the micro-hotplate occurred. To compare the heater's resistivity as a function of the temperature of the four different types of devices, the normalized resistance was chosen instead of the TCR (thermal coefficient of resistance) because the temperature variation between 0 and 120 mW was not accurately known.

The thermal time constant was deduced by measuring the voltage across a resistor connected in series with the heater when a square signal was applied to system. The voltage variation is directly linked to the change in resistance of the heating element, which depends on the temperature of the micro-hotplate. The thermal time constant correspond to the time required to reach the 90% of the steady-state voltage.

3.2.3. Electrical measurements

For each of the two electrical tests made, measurements were performed on 10 samples for each type of devices. The averages and the standard deviations of the results obtained were calculated and used for comparison. First, a quick power ramp was applied to the micro-hotplates in order to identify the maximum power and current density it can withstand before breakdown. The voltage was ramped up from 0 to 10 V, with increments of 50 mV every 100 ms, until breakdown using a *Hewlett-Packard 4155A semiconductor parameter analyzer*.

Second, since such devices can aim at operating for several years before malfunction, reliability of these micro-hotplates is one of the most relevant aspects of this study. Hence, an accelerated aging test was performed to reduce the time before failure to several days instead of several years in the case of a normal operation [6,8]. These devices operated at an input power of 120 mW (685 °C). The voltage applied to the device was monitored throughout this experiment using an *Agilent 34970A data acquisition/switching unit*. By combining the values of the current circulating in the platinum-based heater and of its minimum cross-section area, where the heater line is the narrowest, the maximum current density can be calculated. As the thicknesses were not equal among the different heating elements, comparing results based on current density instead of current is more suitable to compare the devices' performances.

Finally, optical and SEM observations were carried out to investigate and to better understand the failure mechanisms.

4. Results and discussion

4.1. Microstructural, mechanical and electrical properties

Table 1 presents a comparison between the four heater compositions. Their thickness, their resistance, their resistivity as well as the stress value of the platinum films were measured during and at the end of the fabrication process.

Fig. 3 presents SEM pictures of the microstructure at the surface of the four platinum heating elements investigated. Hillocks and voids between the grains were observable. It is assumed to be caused by the deposition of the second low-stress LPCVD Si_xN_y layer, which induced stress and recrystallisation of platinum [15,17,18]. The thickness of the adhesion layer showed

Table 1
Properties of the heaters related to their material composition (the thickness and resistance of the heater after the fabrication are presented as well as the stress and resistivity of the platinum films)

Heater type	Thickness (nm)	R (Ω)	Resistivity (Ω m)	Stress (MPa tensile)
PtTathin	220	91	1.7×10^{-7}	1063
PtTaThick	218	116	2.4×10^{-7}	1062
PtTaSi	207	97	1.7×10^{-7}	1132
IrPtTa	215	167	3.2×10^{-7}	1062

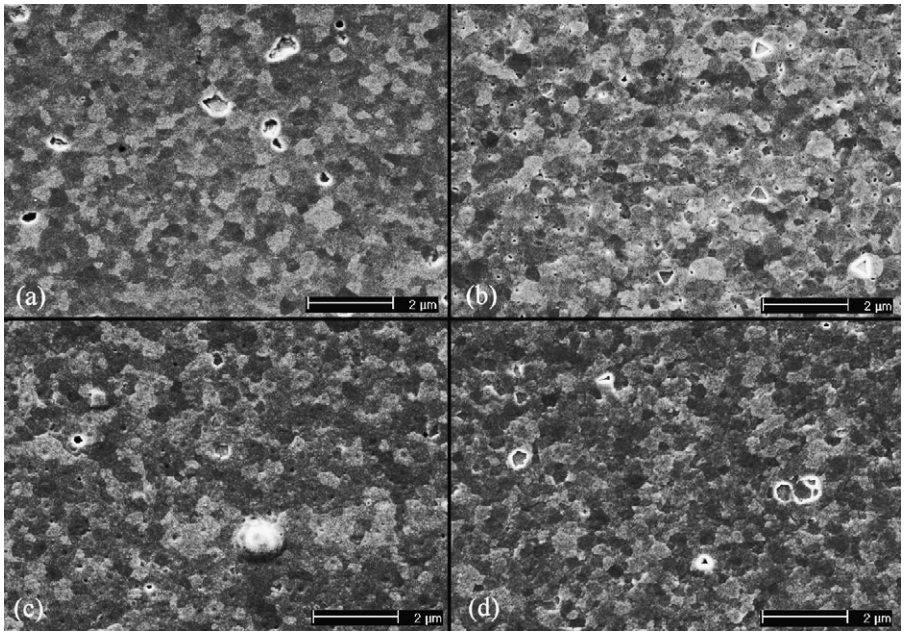

Fig. 3. SEM pictures of the microstructure of platinum at the surface of the heater: (a) PtTaThin; (b) PtTaThick; (c) PtTaSi; and (d) IrPtTa.

an influence on the microstructure, since PtTaThin exhibited more hillocks than PtTaThick. PtTaSi had more hillocks and larger voids between the grains than the three other heating elements and exhibited the roughest surface. This is caused by the formation of tantalum silicides underneath the platinum, which causes a decrease of the layer's thickness due to atom rearrangements. It is well known that the thickness of silicide form is smaller than the addition of the thickness of silicon and tantalum layers used [20]. From the SEM observations, the surface of IrPtTa film presented a smoother microstructure than those of the other materials. Less voids and hillocks were observed for that composition.

After deposition of the platinum, the stress of the films varied in between 600 and 825 MPa. The deposition of the second silicon nitride film induced an increase of the stress to values higher than 1 GPa, with PtTaSi exhibiting the highest stress at 1.13 GPa. This is assumed to be due to the formation of silicides. More voids and hillocks appeared in the platinum line with the procedure consisting in an annealing of the film before the deposition of the second layer of silicon nitride. Poorer results were achieved with the latter. Therefore, only the devices with the salicidation of the Ta that occurred during the deposition of the second layer of Si_xN_y were further studied.

The deposition of the second low-stress LPCVD Si_xN_y layer performed at 800 °C led to a significant modification of the resistivity of the PtTaThick and IrPtTa thin films (Table 2), while those of PtTaThin and PtTaSi only slightly changed. The thickness of the adhesion layer exhibited a noticeable influence on the variation of the platinum films resistivity after the deposition of silicon nitride at high temperature. Previous experiments have shown that interdiffusion between platinum and tantalum occurred only at the interface between the two materials [17] and we can consider its influence on the variation of resistivity to be relatively limited, probably more predominant for the thicker tantalum adhesion layer. In the case of the PtTaThick, nucleation and growth processes happening in the platinum film during silicon nitride deposition are believed to be the main mechanism that increased the resistivity, as reported in references [15,17]. After this processing step, some of the platinum grains had a larger size than the thickness of the film. Voids are created and thus the resistance increased. In contrary, for PtTaThin, neither the interdiffusion between Pt and Ta nor the nucleation and growth processes seems to have an effect on the resistivity of the film. More investigations are definitely needed to explain this difference of behavior. For PtTaSi, a slight increase of the heater resistance was observed even if the tantalum thickness was smaller than for the PtTaThin. We can assume that the tantalum formed tantalum silicides with the silicon and its diffusion in the platinum was limited. However, the small change in resistivity might be due to the stress owning to the formation of the silicide and to its effect on the growth of the platinum grains. As we expected, the resistance of the IrPtTa increased tremendously during this fabrication step due to the diffusion of iridium at the platinum grain boundaries. A resistance increase of about 74% has been measured.

The normalized resistance between 0 and 120 mW, $\Delta R/R_0$, of PtTaThin, PtTaThick, PtTaSi and IrPtTa was, respectively,

Table 2
Influence of the second deposition of low-stress LPCVD Si_xN_y thin film on the heater sheet resistance value

Heater type	Sheet resistance before silicon nitride (Ω/sq)	Sheet resistance after silicon nitride (Ω/sq)
PtTathin	0.79	0.80
PtTaThick	0.86	1.07
PtTaSi	0.83	0.88
IrPtTa	0.86	1.50

125%, 105%, 128% and 61%. It is observable this ratio is linked to the composition of the heating element. By having the same thickness of platinum, PtTaThin and PtTaSi presented an almost identical change in resistance, whereas PtTaThick showed a lower variation. Addition of iridium at the grain boundaries of the platinum decreased significantly this ratio.

4.2. Mechanical deformation during operation

During operation, two modes of deformations were observed. An asymmetrical mode occurred at a power below 80 mW while a symmetrical shape was observable at higher power (Fig. 4). The power threshold between these modes depended on the heater materials used, between 80 and 85 mW for PtTaThick, PtTaSi and IrPtTa, and between 95 and 100 mW for PtTaThin. At high power, IrPtTa bended downwards while the other heating elements generally bended upwards. This phenomenon clearly linked the heater composition since the thickness of the two silicon nitride layers composing the membrane was identical for all the devices. However, the amplitude of deformation only had a slight dependence on the materials. At a power of 120 mW, the symmetrical deformation of IrPtTa was 11 μm, while that of the three other heating devices was 12 μm. Since the input power of the four different devices was the same, one can deduce that the amplitude of deformation is more likely linked to the thermal expansion of the membrane due the temperature difference between the stacked materials forming the membrane and the silicon bulk, which stays at room temperature.

4.3. Maximum power leading to breakdown

The second test performed to characterize the reliability of these devices was the determination of the maximum power the micro-hotplate can withstand before failure occurs. Since the thermal time constants of the heating elements were determined to be between 10 and 20 ms, the time delay of 100 ms between each step of the applied voltage ramp ensured that the devices

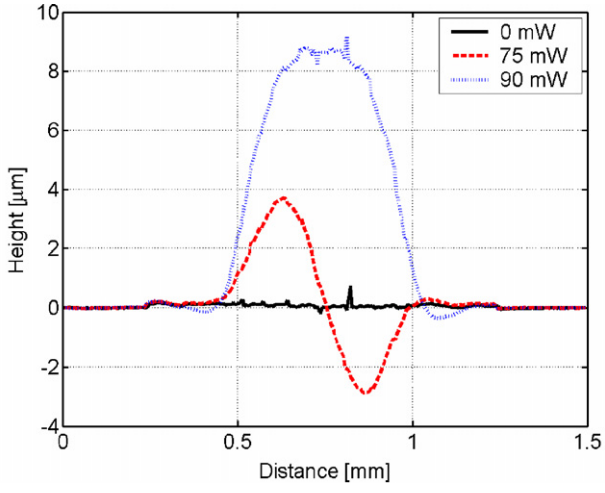

Fig. 4. Deformation of PtTaSi heating element. The membrane was flat at 0 mW. Asymmetrical and symmetrical shapes were observed at 75 and 90 mW, respectively.

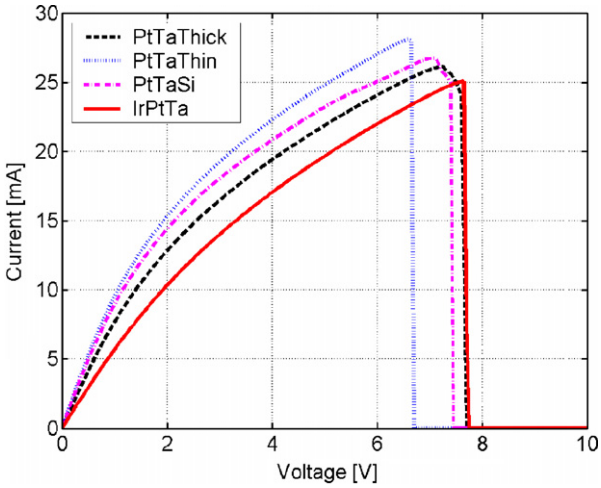

Fig. 5. Results of the maximum power test leading to breakdown. Voltage was ramped up by 50 mV every 100 ms. IrPtTa reached the highest power, 197 mW.

reached their thermal equilibrium before increasing the voltage to its next value. The results obtained are presented in Fig. 5 and summarized in Table 3. PtTaThin reached the highest current density due to its lower resistance compared to the other heaters. A similar result was obtained with PtTaSi. However, the best performance was exhibited by IrPtTa, which reached the highest power and, hence, the highest temperature before breakdown. In addition, the reproducibility of the results was excellent regarding to the standard deviation of each type of heating element, which was always below 1% of the average value of the maximum power reached. As aforementioned, the mechanical deformation was similar for all the heating elements at a given power when they reach the symmetrical shape, but by having a higher resistance IrPtTa required less current to reach the given power and electro-stress migration was thus delayed.

4.4. Accelerated aging

With the aim of reducing the time before the failure of the heating devices, from several years in the case of their normal operation to some days, an accelerated aging test was carried out at a constant input power of 120 mW. The results are presented in Table 4. The longest life span, 3.8 days, was exhibited by IrPtTa type of device. This result was expected since the resistance value of this heater was the highest at 120 mW. Despite its smaller TCR compared to the other heating elements, a lower current density was required to reach the predefined power, delaying thus the electro-stress migration. The thickness of

Table 3
Results of the maximum power test (the voltage was ramped up from 0 to 10 V with steps of 50 mV every 100 ms. The highest current density and the highest power were withstood by PtTaThin and IrPtTa, respectively)

Heater type	P_{max} (mW)	σ (mW)	J_{max} (A/cm^2)
PtTaThin	186.2	1.6	4.29×10^5
PtTaThick	191.5	0.8	3.75×10^5
PtTaSi	186.7	0.9	4.19×10^5
IrPtTa	196.0	0.9	3.94×10^5

Table 4
Parameters of the device that performed the accelerated aging test (average resistance value at room temperature and at 120 mW, maximum current densities at 120 mW, the percentage of the resistance drift per day, the number of days operating at 120 mW and their standard deviation. The narrowest part of the heater was 30 μm wide)

Heater type	R_{RT} (Ω)	$R_{120\,mW}$ (Ω)	$J_{120\,mW}$ (A/cm^2)	Drift (%/day)	Days	σ (day)
PtTaThin	91	205	3.67×10^5	8.2	0.7	0.2
PtTaThick	116	239	3.43×10^5	5.9	1.8	0.2
PtTaSi	97	221	3.77×10^5	10.0	0.6	0.3
IrPtTa	167	270	3.26×10^5	3.9	3.8	1.1

the adhesion layer showed a strong influence on the lifetime. PtTaThick broke after 1.8 days and PtTaThin after only 0.7 day. Moreover, by taking into account the standard deviation measured, one can see that the IrPtTa type of heater, even in the worst case, exhibited better performance than the best result obtained with PtTaThick heating elements. In relation with the initial resistance at 120 mW, the average resistance drifts during accelerated aging for PtTaThin and PtTaThick were 8.2% and 5.9% per day. IrPtTa exhibited the lowest resistance drift, which was 3.9% per day.

The formation of tantalum silicides did not improve the reliability of the devices. Due to its low resistivity and despite having a slightly larger variation of its resistance between 0 and 120 mW, PtTaSi still required the highest current density to reach 120 mW. This type of heater exhibited the poorest performance with a breakdown occurring after 0.6 day and a drift of its resistance value of 10.0% per day at 120 mW. The large amount and the large size of the hillocks and voids that appeared in the PtTaSi microstructure compared to the other devices, combined with a probable unsatisfactory quality of tantalum silicides, might speed up the electro-stress migration effect, leading more rapidly to failure. An improvement of this layer might be obtained by using co-evaporation of Si and Ta or another deposition method than e-beam evaporation, such as the sputtering of a $TaSi_x$ target.

One can see that the lifetime of the devices was directly related to the current density. The lower the current density, the longer was the life span. Consequently, the resistivity at the operating temperature has to be maximized so as to decrease as most as possible the current density and thus delaying electro-stress migration. The resistivity at room temperature has to be as high as possible and the TCR as well. IrPtTa filled the first condition and despite having a small TCR it still exhibited the highest resistivity at 120 mW compared to the three other heating elements. It thus showed the best performances throughout this test.

For their typical application in the gas sensing field, such devices will be heated up to about 300 °C, corresponding to a power of about 45 mW. Therefore, at that lower power, the influence of the TCR is less significant and the difference of resistivity between IrPtTa and the three other types of micro-heating elements is larger than at 120 mW. Consequently, an IrPtTa heater will require a much smaller current density to reach that input power compared to the other devices, which we could expect to extend even more the lifetime of the device at lower temperature.

4.5. Failure analysis investigation

Finally, failure analysis has been carried out in order to better understand the main breakdown mechanisms. Two failure modes were observed for both reliability tests performed in this study, electro-stress migration of the platinum forming the heater and breaking of the membrane.

Concerning the maximum power test leading to breakdown, the two failure modes were clearly linked to the heater composition. Failure of PtTaThick was only due to breaking of the membrane while in PtTaThin and IrPtTa only electro-stress migration arose. In the case of PtTaSi, both modes of failure occurred. The current and the deformation of the membrane induced stress with a non-uniform distribution that had a strong influence on the location of the failure in the case of the electro-stress migration. The stress has its origin in the mismatch of the thermal coefficient of expansion (TCE) of the stacked materials and the non-uniform temperature over the membrane [24]. This type of failure always occurred in the same zone at a localized place, where the combination of temperature, level of stress and current density are assumed to favor the migration of the platinum atoms (Fig. 6). The zone where the failure happened

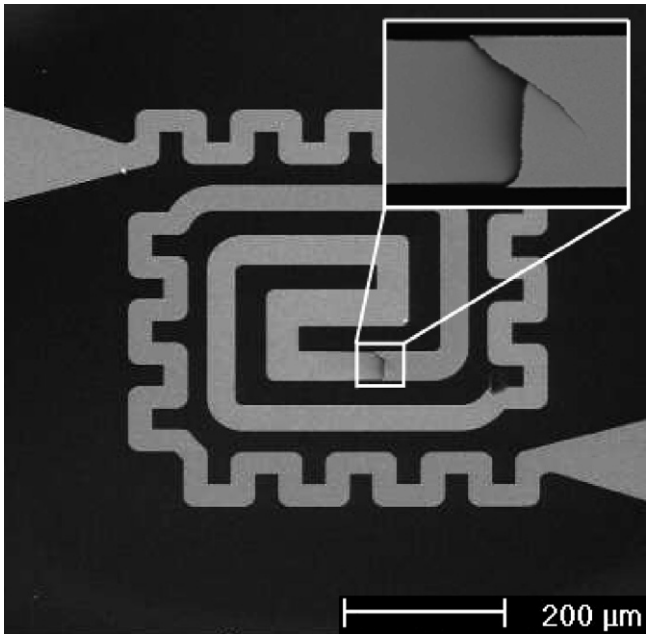

Fig. 6. SEM picture showing the breakdown of an IrPtTa heater due to electro-stress migration. The voltage was ramped up by 50 mV every 100 ms. Failure occurred at an input power of 197 mW.

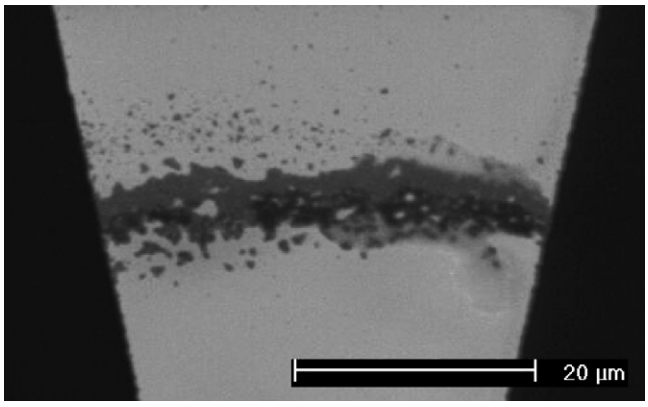

Fig. 7. SEM picture showing the breakdown due to electro-stress migration at the junction of the interconnection and the heating element of a PtTaThin device during the accelerated aging test at 120 mW.

was more localized than in the case of the accelerated aging test, certainly due to the fast and constant increase in the input power as well as the larger deformation reached compared to the accelerated aging test.

During the accelerated aging test, electro-stress migration was observed with the four heater compositions and was the predominant failure mechanism [10]. Moreover, the breaking of the membrane was observed for almost all micro-hotplates, sometimes several days after failure of the heating element occurred. This is a consequence of the electro-stress migration that caused highly localized stress in different regions of the hotplate, weakening the mechanical robustness of the membrane. In the case of the electro-stress migration, a wide discontinuity in the platinum heater clearly appeared as shown in Fig. 7. The localization of this phenomenon between the interconnection line and the heating element in itself was not observable throughout the test where the voltage was ramped up. Atoms in the negative part of the conductor migrate in the direction of the electron flow and to the region where the temperature is higher [25]. Since failure occurred at the edge of the heating element, where the temperature gradient is significant, the thermal gradient might have also contributed to the failure of the heating element, but the importance of this contribution still needs to be evaluated.

5. Conclusion

Enhancement of micro-hotplates' performances by modifying the platinum-based heater material composition has been demonstrated. Maximum power leading to breakdown of the device and accelerated aging tests have shown that addition of iridium increased the resistance of the heating element and thus decreased the current density required to reach a given temperature. By minimizing the current density, the electro-stress migration is delayed and, consequently, the life expectancy and thus the reliability of the micro-hotplate are improved.

Optical and SEM pictures helped us to better understand the failure mechanism. Electro-stress migration was responsible for the breakdown of these devices. However, depending on the type of test performed, this phenomenon did not occur at the same place on the heating area and the location did not seem to be material dependant.

Further experiments will be carried out to better understand the failure mechanisms. Electromigration tests at constant current density and temperature will be performed on devices without membrane to avoid the influence of the deformation on the failure of the heater. Such a test will allow examining the influence of the addition of iridium on the delay of electromigration.

Acknowledgements

We would like to thank the IMT-COMLAB technical staff for their support in the fabrication of the devices.

References

[1] P.M. Sarro, A.W. Van Herwaarden, W. Van der Vlist, A silicon–silicon nitride membrane fabrication process for smart thermal sensors, Sens. Actuators A41–A42 (1994) 666–671.
[2] I. Simon, N. Barsan, M. Bauer, U. Weimar, Micromachined metal oxide gas sensors: opportunities to improve sensor performance, Sens. Actuators B73 (2001) 1–26.
[3] W. Konz, J. Hildenbrand, M. Bauersfeld, S. Hartwig, A. Lambrecht, V. Lehmann, J. Wöllenstein, Micromachined IR-source with excellent blackbody like behaviour, Proc. SPIE vol. 5836 (2005) 540–548.
[4] C. Rossi, D. Briand, M. Dumonteuil, T. Camps, P.Q. Pham, N.F. de Rooij, Matrix of 10 × 10 addressed solid propellant microthrusters: review of the technologies, Sens. Actuators A126 (1) (2006) 241–252.
[5] D. Briand, S. Heimgartner, M.-A. Gertillat, B. van der Schoot, N.F. de Rooij, Thermal optimization of micro-hotplates that have a silicon island, J. Micromech. Microeng. 12 (2002) 971–978.
[6] J.-M. Bosc, Y. Guo, V. Sarihan, T. Lee, Accelerated life testing for microchemical sensors, IEEE Transactions on Reliability 47 (2) (1998) 135–141.
[7] D. Briand, S. Heimgartner, M. Dadras, N.F. de Rooij, On the reliability of a platinum heater for micro-hotplates, in: Proc. of Eurosensors XVI, Prague, Czech Republic, 2002, pp. 474–477.
[8] D. Briand, G.-M. Tomassone, N.F. de Rooij, Accelerated ageing of micro-hotplates for gas sensing applications, in: Proc. of IEEE sensors conference, Toronto, Canada, 2003, pp. 1314–1317.
[9] J. Puigcorbé, D. Vogel, B. Michel, A. Vilà, I. Gràcia, C. Cané, J.R. Morante, Thermal and mechanical analysis of micromachined gas sensors, J. Micromech. Microeng. 13 (2003) 548–556.
[10] D. Briand, F. Beaudoin, J. Courbat, N.F. de Rooij, R. Desplats, P. Perdu, Failure analysis of micro-heating elements suspended on thin membranes, Microelectronic Reliability 45 (2005) 1786–1789.
[11] M. Ehmann, P. Ruther, M. von Arx, O. Paul, Operation and short-term drift of polysilicon-heated CMOS microstructures at temperature up to 1200 K, J. Micromech. Microeng. 11 (2001) 397–401.
[12] O. Grudin, R. Marinescu, L. Landsberger, D. Cheeke, M. Kahrizi, Microstructure release and test techniques for high-temperature micro hotplate, in: Proceedings of IEEE Canadian Conference on Electrical and Computer Engineering, vol. 3, no. 9, May 12, 1999, pp. 1610–1615.
[13] M. Graf, D. Barrettino, K.-U. Kirstein, A. Hierlemann, CMOS microhotplate sensor system for operating temperatures up to 500 °C, Sens. Actuators B117 (2006) 346–352.
[14] T. Maeder, L. Sagalowicz, P. Muralt, Stabilized platinum electrodes for ferroelectric film deposition using Ti, Ta and Zr adhesion layers, Jpn. J. Appl. Phys. 37 (1998) 2007–2012.
[15] S.L. Firebaugh, K.F. Jensen, M.A. Schmidt, Investigation of high-temperature degradation of platinum thin films with an in situ resistance measurement apparatus, J. Microelectromechanical Systems 7 (1) (1998) 128–135.
[16] H. Esch, G. Huyberechts, R. Mertens, G. Maes, J. Manca, W. De Ceuninck, L. De Schepper, The stability of Pt heater and temperature sensing elements

for silicon integrated tin oxide gas sensors, Sens. Actuators B65 (2000) 190–192.

[17] D. Briand, S. Heimgartner, M. Leboeuf, M. Dadras, N.F. de Rooij, Processing influence on the reliability of platinum thin films for MEMS applications, in: MRS Symposium Proceedings vol. 729, BioMEMS and Bionanotechnology, San Francisco, CA, USA, April 2002, 2002, pp. 63–68.

[18] R.M. Tiggelaar, J.W. Berenschot, J.H. de Boer, R.G.P. Sanders, J.G.E. Gardeniers, R.E. Oosterbroek, A. van den Berg, M.C. Elwenspoek, Fabrication and characterization of high-temperature microreactors with thin film heater and sensor patterns in silicon nitride tubes, Lab. Chip 5 (2005) 326–336.

[19] U. Schmid, H. Seidel, Enhanced stability of Ti/Pt micro-heaters using a-SiC:H passivation layers., Sens. Actuators A130–A131 (2006) 194–201.

[20] S.P. Murarka, Silicide for VLSI Applications, Academic Press, New York, 1983.

[21] T. Massalski (Ed.), Binary Alloy Phase Diagrams, vol. 2, American Society for Metals, 1986, p. 2224.

[22] D. Briand, A. Krauss, B. van der Schoot, U. Weimar, N. Barsan, W. Göpel, N.F. de Rooij, Design and fabrication of high-temperature micro-hotplates for drop-coated gas sensors, Sens. Actuators B68 (2000) 223–233.

[23] L. Thiery, D. Briand, A. Odaymat, N.F. de Rooij, Contribution of scanning probe temperature measurements to the thermal analysis of micro-hotplates, in: International Workshops on Thermal Investigations of ICs and Systems, Therminic 2004, Sophia Antipolis, France, September 2004, 2004, pp. 23–28.

[24] J. Puigcorbé, A. Vilà, J. Cerdà, A. Cirera, I. Gràcia, C. Cané, J.R. Morante, Thermo-mechanical analysis of micro-drop coated gas sensors, Sens. Actuators A97–A98 (2002) 379–385.

[25] M. Ohring, Reliability and Failure of Electronic Materials and Devices, Academic Press, New York, 1998.

Biographies

J. Courbat received his MSc degree in microtechnology from the Swiss Federal Institute of Technology, Lausanne (EPFL) in 2005. He currently works as a PhD student in the Institute of Microtechnology, University of Neuchâtel, Switzerland. His research activities are focused on the integration of gas sensors on flexible substrates.

D. Briand received his BEng degree and MASc degree in engineering physics from École Polytechnique in Montréal, in collaboration with the Laboratoire des Matériaux et du Génie Physique (INPG) in Grenoble, France, in 1995 and 1997, respectively. He obtained his PhD degree in the field of micro-chemical systems from the Institute of Microtechnology, University of Neuchâtel, Switzerland, in 2001, where he is currently a project leader. He is in charge of European and industrial projects and of the supervision of doctoral students. His research interests in the field of microsystems include PowerMEMS, polymeric MEMS, the integration of nanostructures on microsystems, and the development of microanalytical instruments for gas-sensing applications.

N.F. de Rooij received a PhD degree from Twente University of Technology, The Netherlands, in 1978. From 1978 to 1982, he worked at the Research and Development Department of Cordis Europa N.V., The Netherlands. In 1982, he joined the Institute of Microtechnology of the University of Neuchâtel, Switzerland (IMT UNI-NE), as professor and head of the Sensors, Actuators and Microsystems Laboratory. Since October 1990 till October 1996, he was acting as director of the IMT UNI-NE. Since 1987, he has been a lecturer at the Swiss Federal Institute of Technology, Zurich (ETHZ), and since 1989, he has also been a professor at the Swiss Federal Institute of Technology, Lausanne (EPFL). His research activities include microfabricated sensors, actuators and microsystems.